CALCULATION ACCURACY OF MATHEMATICAL HOMOGENIZATION METHOD FOR THERMO-MECHANICAL COUPLING PROBLEMS

by

Jianxia GUO*

School of Mathematics and Statistics, Xinxiang University, Xinxiang, Henan, China

Original scientific paper
https://doi.org/10.2298/TSCI2104957G

The paper analyzes the thermo-mechanical couplinag phenomenon under the condition of sliding contact, establishes the finite element analysis continuous model of thermo-mechanical coupling, and proposes the system dynamic equilibrium equation and thermodynamic equilibrium equation. The article analyzes the contact conditions between the objects in the system and obtains the objects' contact conditions' mathematical expression. On this basis, the constraint function is used to express the mathematical homogenization. We apply the variation principle to the constraint function and form a non-linear equation group with the system balance equation solve the thermal-mechanical coupling problem. The example shows that we use the constraint function method to solve the thermo-mechanical coupling problem, which has good convergence, stable algorithm, and the calculation result can reflect the actual situation.

Key words: *thermal-mechanical coupling, constraint function method, mathematical homogenization method, calculation accuracy*

Introduction

One of the difficulties in thermal-mechanical coupling analysis under slip contact conditions is determining the temperature field changes of the analysis model due to slip contact friction, such as cutting processing, sheet metal stamping forming, and brake systems*, etc.* Temperature changes impact processing accuracy, forming, the braking effect*, etc.* have a significant influence. This coupling of heat transfer and mechanics shows prominent non-linear characteristics: non-linear heat transfer and non-linear contact. The results of mechanical calculations affect the calculations of thermodynamics. Similarly, the estimates of thermodynamics will also affect the calculations of mechanicals [1]. Based on the research on the mechanism of object heating caused by sliding frictional contact between objects, some scholars pointed out that the number of contact surfaces, relative spatial position, and slip rate play a vital role in heating.

Thermal-mechanical coupling analysis is a highly non-linear process, and the contact conditions show strong non-linearity. Generally, the Lagrange multiplier method, penalty function method, disturbance Lagrange method, and incremental Lagrange method deal with frictional contact constraints. For multi-object friction contact, the mathematical homogenization method proposes a new friction time integration algorithm. The mathematical homogenization method proposes a new contact element based on the penalty function method. Its advantage is that the contact element stiffness matrix is symmetric. The same applies to the massive slip problem of frictional contact.

* Author's e-mail: guojianxia2006@163.com

The mathematical homogenization method analyzes the existing methods of dealing with contact problems and proposes the constraint function method. This method has good convergence and robustness [2]. Compared with other methods, the constraint function method has certain advantages through some example analysis and comparison. In this paper, based on Bathe's constraint function method, a thermo-mechanical coupling model is established. The constraint function method is applied to deal with the thermo-mechanical coupling problem by analysis of contact conditions.

Thermo-mechanical coupling model

Generally speaking, three main factors cause the problem of thermal coupling between objects: the internal heat caused by the plastic deformation of the material; the heat exchange of the contact body; the contact surface generates a surface heat source due to the friction the contact surface between the objects. Without loss of generality, the article assumes that the system is composed of M objects $\wp^I$ ($I = 1..., M$). The volume of the object $\wp^I$ at time t is denoted as ${}^tV^I$ and is at $t \in [0, T]$. For any $I \neq J$, there is ${}^tV^I \cap {}^tV^J = \phi$, fig. 1. Applying the principle of virtual work, the system dynamics balance equation:

$$\sum_{I=1}^{M} \int {}^0V^I S^{\circ} \delta\varepsilon \mathrm{d}{}^0V^I =$$

$$= \sum_{I=1}^{M} \int {}^0V^I \rho(f^B - \ddot{u}\delta_{ll}\mathrm{d}{}^0V^I) + \int {}^{\partial 0}V_f^I f^S \circ \delta_{ll}\mathrm{d}{}^{\partial^0}V_f^I + \int {}^{\partial 0}V_f^I fc \circ \mathrm{d}u\mathrm{d}\partial V_f^I \tag{1}$$

where ρ is the density and δu – the virtual displacement [3]. The thermodynamic effect of friction impacts the system in the dynamic equilibrium equation so the design must consider the thermodynamic equilibrium equation. Therefore, according to the first law of thermodynamics or the principle of thermal energy balance, the system thermodynamic balance equation can be written in the variational form:

$$\sum_{I=1}^{M} \int {}^0V^t \rho c \partial_t \theta \delta\theta \mathrm{d}{}^0V^I = \sum_{I=1}^{M} \left\{ \int {}^0V^I Q_M \delta\theta \mathrm{d}{}^0V^I - \int {}^0V^I k \mathrm{grad}(\theta)^{\circ} \mathrm{grad}(\delta\theta)\mathrm{d}{}^0V^I + \right.$$

$$\left. + {}^0V^I \rho q^B \delta\theta \mathrm{d}{}^0V^I + \int {}_{\partial 0}V_q^I q_e^{s\circ} \delta\theta \mathrm{d}\partial^0 V_q^I + \int \partial^t V_q^I qc^{\circ} \delta\theta \mathrm{d}^{\partial^t} V_q^I \right\} \tag{2}$$

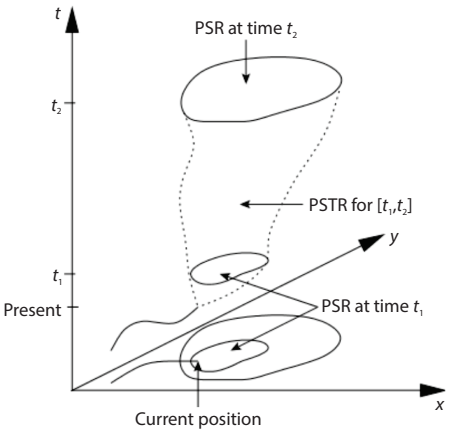

Figure 1. Contact model between objects, *t*

where θ is the temperature field, c and k – the heat capacity coefficient and thermal conductivity coefficient, respectively, Q_M – the force coupling term, q^B, q_e^s , q^c are the internal heat generation rate, the heat flow acting on the surface of the object, and the heat flow generated by the contact action, respectively: force the coupling term Q_M essentially represents the internal heat generated by plastic deformation in a unit volume:

$$Q_M = \omega\bar{\tau} \circ \overline{D^p} \tag{3}$$

where $\bar{\tau}$ is the Cauchy stress tensor and $\bar{D}^p$– the plastic strain rate tensor, they are all tensors relative to the midplane, and ω represents the thermal energy loss rate ($0 \leq \omega \leq 1$). Figure 1, S^{IJ} and S^{JI} are the

surfaces where objects I and J may come into contact and are called contact pairs, and Sc is the surfaces where they contact each other, namely: $Sc \in S^{IJ} \cap S^{JI}$. Therefore, the system contact pair set C can be expressed as: $C = \{(S^{IJ}, S^{JI}): I \neq J\} n^J$ and S^J are the normal and tangential directions of the contact surface at the contact point, f_{nc} is the component of the moderate approach of the contact pressure, and f_{tc} – the tangential component of the contact pressure acting on the object I.

Contact analysis

Contact conditions

In applying the finite element method to the analysis of object contact, it is usually assumed that the contact surface is smooth. But in reality, the contact surface is often non-smooth, especially when considering the contact objects' heat conduction. The geometric characteristics of the contact surface are fundamental [4]. The heat conduction analysis of the contact surface is shown in fig. 2. In fig. 2, g is the gap function. Let X^I be the co-ordinate of any point on S^{IJ}, and $X^I \in S^{IJ}$, if it satisfies:

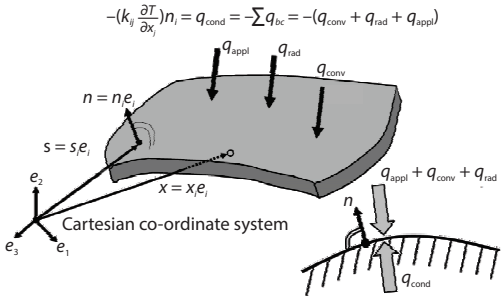

Figure 2. Thermal conductivity analysis model of the contact surface

$$-\left(k_{ij}\frac{\partial T}{\partial x_j}\right)n_i = q_{\text{cond}} = -\sum q_{bc} = -\left(q_{\text{conv}} + q_{\text{rad}} + q_{\text{appl}}\right)$$

$$\left\|X^I - X^J\right\|_2 = \min_{X^J \in S^{JI}}\left\{\left\|X^I - X^J\right\|_2\right\} \tag{4}$$

Then the gap function, g, can be written:

$$g = \left(X^I - X^J\right)^T n^J \tag{5}$$

In the case of no penetration at the contact surface, obviously $g \geq 0$. According to general regulations, normal contact pressure $f_{nc} \geq 0$. At the contact point, be $g > 0$, $f_{nc} = 0$, and $g = 0$ be $f_{nc} > 0$. The previous analysis can be obtained that, regardless of penetration, the contact conditions between objects in the average direction of the object's surface can be expressed as follows. Therefore, normal contact conditions are shown in fig. 3.

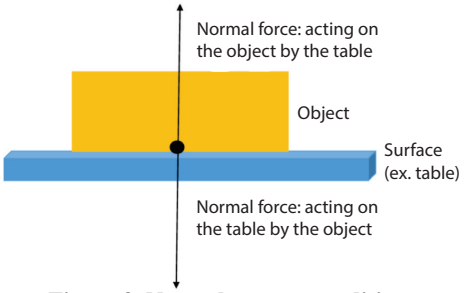

Figure 3. Normal contact conditions

$$g \geq 0, f_{nc} \geq 0, g^{\circ} f_{nc} = 0 \tag{6}$$

In the contact situation, let ζ be a dimensionless variable, and ζ is defined:

$$\zeta = \begin{cases} \dfrac{f_{tc}}{F_r}(F_r \neq 0) \\ 0 \end{cases} \tag{7}$$

where F_r is the friction resistance and $F_r = \mu f_{nc}$ and μ – the friction coefficient. There are two possibilities for the state of motion of the contacting object under the action of various force systems: relative slip and static [5]. If the relative slip tangential velocity is defined:

$$\bar{v} = (v^J \circ v^I) \circ S^J \tag{8}$$

where v^I and v^J are the speed of object I and object J at the contact point. Slip condition: if $\bar{v} \neq 0$ then $|f_{tc}| = F_r$. According to eq. (7), $|\zeta| = 1$ is obtained. No-slip condition: if $\bar{v} = 0$, then $|f_{tc}| \leq F_r$, so $|\zeta| \leq 1$.

According to the aforementioned two states, the friction contact condition based on Coulomb's law can be obtained:

$$|\zeta \leq 1| \tag{9}$$

Suppose that $\bar{v} > 0$ is then $v^I \circ S^J > v^I \circ S^J$, so f_{tc} and $\bar{v}$ acting on the object I are in the same direction. It can be seen that when $|\zeta| = 1$ is $\text{sign}(\bar{v}) = \text{sign}(\bar{v})$. From the previous analysis, it can be seen that the friction contact condition can be written:

$$\begin{gathered} |\zeta| \leq 1 \\ |\zeta| < 1 \Rightarrow \bar{v} = 0 \\ |\zeta| = 0 \Rightarrow \text{sign}(\bar{v}) = \text{sign}(F_r) \end{gathered} \tag{10}$$

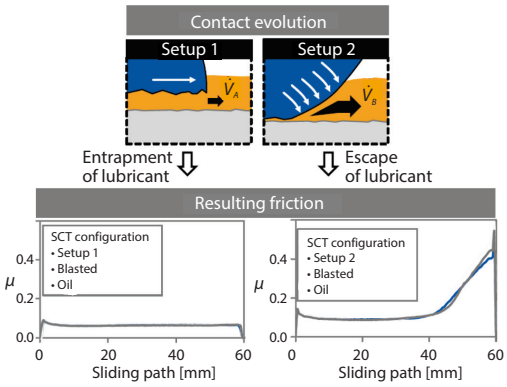

Figure 4. Friction contact conditions

The friction contact conditions are shown in fig. 4. From the previous analysis of the contact conditions, it can be seen that the conditional eq. (6) indicates whether the objects are in contact; the conditional eq. (10) shows whether the objects in the contact state slip due to friction, that is, the friction contact condition.

Contact items

On the contact surface, the contact force due to contact can be expressed:

$$f_c^I = f_{nc} n^J + f_{tc} S^J \tag{11}$$

Let $\Delta\delta_u^{IJ} = \delta_u^I - \delta_u^J$ be the virtual displacement of an object I relative to a thing J, so the contact term in eq. (1) can be written:

$$\sum_{k=1}^{M} \int \partial t V_f^k f \circ \delta_u \mathrm{d}\partial^t V_f^k = \sum_{(S^U, S^{JI}) \in C} \int_{S_C} \left(f_{nc} n^J + f_{tc} S^J \right) \circ \Delta\delta_u^{IJ} \mathrm{d}S_c \tag{12}$$

On the unit contact surface area, the heat generated due to frictional slip can be expressed:

$$q_G^{IJ} = \gamma f_{tc} \bar{v} \tag{13}$$

where γ is a coefficient considering heat loss. Applying the First law of thermodynamics can be derived:

$$q_c^I + q_c^J - q_G^{IJ} = 0 \tag{14}$$

where

$$q_c^I = h(\theta^J - \theta^I) + q_G^I \tag{15}$$

$$q_c^J = h(\theta^I - \theta^J) + q_G^J \tag{16}$$

where h is the thermal conductivity of contact related to material properties, geometric characteristics of the contact surface, contact pressure, *etc.* The first term on the right side of eqs. (15) and (16) represents the heat exchange caused by the different surface temperature of the contact object, and the second term represents the heat transfer due to contact friction the parts of other contact objects [6-8]. Therefore, the last term of eq. (2) can be written:

$$\sum_{k=1}^{M}\int \partial^t q_c \circ \delta\theta \mathrm{d}\partial^t V_q^I = \sum_{(S^{IJ},S^{JI})\in C}\left\{\int s_c h \circ \Delta\delta\theta^{IJ}\mathrm{d}S_c + \int s_c q_G^I \delta\theta^I \mathrm{d}S_c + \int s_c q_G^J \delta\theta^J \mathrm{d}S_c\right\} \tag{17}$$

Constraint function

In contact analysis, there are many ways to deal with contact conditions. This article adopts the constraint function method. The following constraint equations can express the contact conditions (6) and (10):

$$\begin{aligned} w_n(g, f_{\mathrm{nc}}) &= 0 \\ w_s(\bar{v}, \zeta) &= 0 \end{aligned} \tag{18}$$

where w_n and w_s are continuously differentiable functions defined by parameters g, f_{nc} and $\bar{v}$, ζ, respectively. The specific form of the function:

$$w_n = \frac{f_{\mathrm{nc}} + g}{2} - \sqrt{\left(\frac{g - f_{\mathrm{nc}}}{2}\right)^2 + \varepsilon_n} \tag{19}$$

$$w_s + \zeta - \frac{2}{\pi}\arctan\left(\frac{\bar{v} - w_s}{\varepsilon_s}\right) = 0 \tag{20}$$

where ε_n and ε_s are any small positive numbers. To verify whether eqs. (19) and (20) satisfy conditional eqs. (6) and (10), according to eq. (18), ε_n takes 0.1 and 0.01, respectively, by calculating eq. (19), the result is shown in fig. 5. Using the same method for eq. (20), the result is shown in fig. 6.

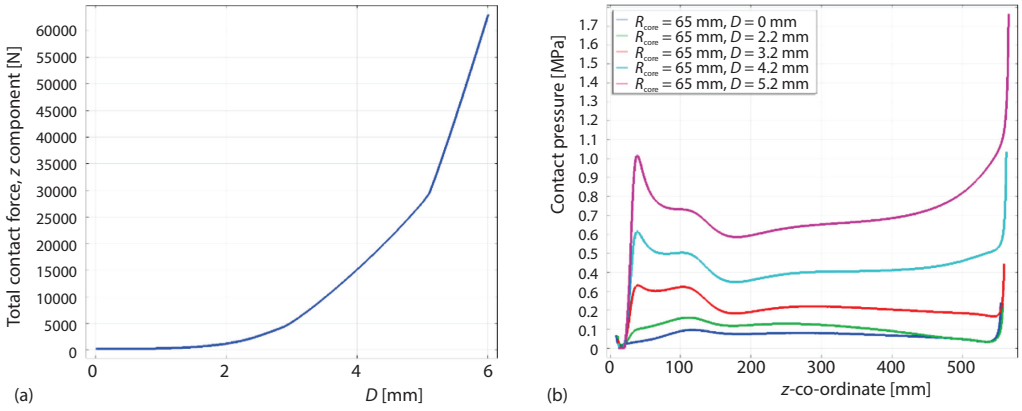

Figure 5. Normal phase contact pressure of eq. (19)

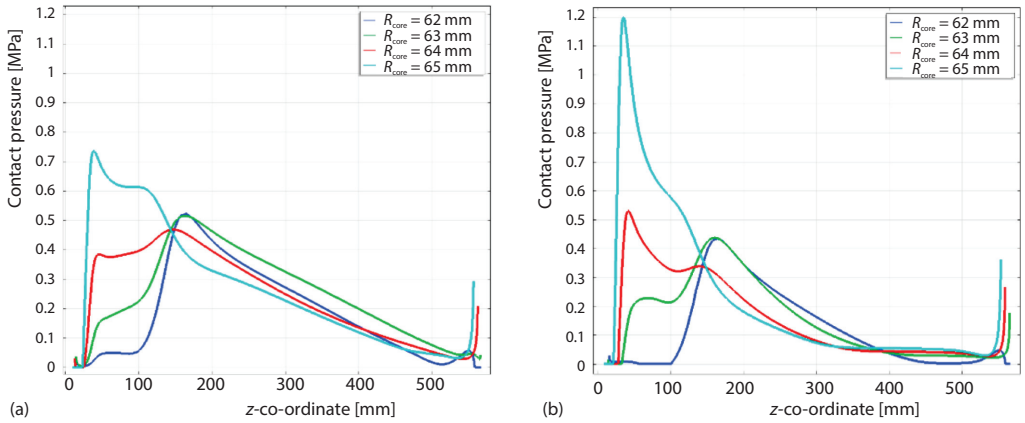

Figure 6. The relative migration tangential velocity of eq. (20)

It can be seen that when $\varepsilon_n \to 0$, eq. (19) satisfies the contact condition eq. (6), fig. 5 is also consistent with fig. 3. The $\varepsilon_s \to 0$ eq. (20) meets the contact condition equation (10), fig. 6 is consistent with fig. 4. The constraint eq. (18) can be written:

$$\int s_c [w_n \delta f_{nc} + w_s \delta \zeta] \mathrm{d}S_c = 0 \tag{21}$$

There is such a constraint equation for every contact pair in the system. The system finite element equation can be written:

$$M^{t+\Delta t}\ddot{u} + {}^{t+\Delta t}F_u = {}^{t+\Delta t}F - {}^{t+\Delta t}F_c \tag{22}$$

$$C^{t+\Delta t}\dot{\theta} + {}^{t+\Delta t}Q_\theta = {}^{t+\Delta t}Q - {}^{t+\Delta t}Q_c \tag{23}$$

$${}^{t+\Delta t}W_c = 0 \tag{24}$$

where F_u, F_c, Q_θ, and Q_c is a function of u, θ, and ζ, where

$${}^{t+\Delta t}\zeta^T = [{}^{t+\Delta t}f_{\mathrm{nc}}^1, {}^{t+\Delta t}\zeta_1, L\cdots, {}^{t+\Delta t}f_{\mathrm{nc}}^k, {}^{t+\Delta t}\zeta, L\cdots, {}^{t+\Delta t}f_{\mathrm{nc}}^m, {}^{t+\Delta t}\zeta_m] \tag{25}$$

Contact condition item ${}^{t+\Delta t}W_c$:

$${}^{t+\Delta t}W_c^T = [{}^{t+\Delta t}W_1^{cT}, L\cdots, {}^{t+\Delta t}W_m^{CT}] \tag{26}$$

where

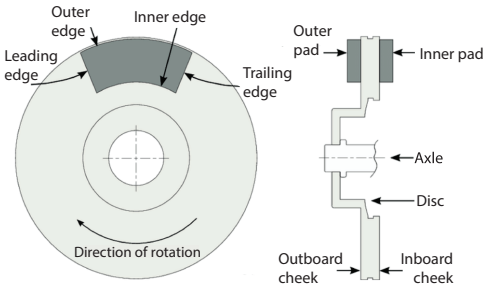

Figure 7. Simplified diagram of disc brake

$${}^{t+\Delta t}W_k^c = \begin{bmatrix} w_n\left({}^{t+\Delta t}g_k, {}^{t+\Delta t}f_{\mathrm{nc}}^k\right) \\ w_s\left({}^{t+\Delta t}\overline{v}_k, {}^{t+\Delta t}\zeta_k\right) \end{bmatrix} \tag{27}$$

where m represents the number of contact points on the contact surface is the number of Gaussian integration points on the contact surface in the calculation [9]. The non-linear equations formed by eqs. (22)-(24) can be solved by the complete Newton-Raphson algorithm to obtain the corresponding displacement, pressure, temperature, and contact variables f_{nc} and ζ.

Numerical examples

The automobile brake system is a typical thermal coupling phenomenon. The hydraulic system pushes the brake pads to press on the brake disc to achieve deceleration. The brake disc absorbs most of the heat generated by the friction between the brake disc and the brake pad. If the temperature is too high in the braking process, it will seriously affect the braking effect, so the brake's climate is not comfortable to be too high during operation [10]. Take the disc brake as an example to illustrate the constraint function method's application solving the thermal coupling problem. The brake system can be simplified, as shown in fig. 7.

Assuming that the brake materials are all thermoelastic isotropic materials, the piston's pressure is 2 MPa, and the initial temperature is both 20°, the brake can exchange heat with the outside world. The brake disc's initial speed is 1200 pm, and the speed is 0 after 6 seconds under braking. The whole-time history of analysis and calculation is 12 seconds.

Figure 8 shows the temperature change of the brake disc surface over the entire time history. It can be seen from figs. 9 and 10 that most of the heat flows to the brake disc, which makes the temperature of the brake disc rise quickly [11].

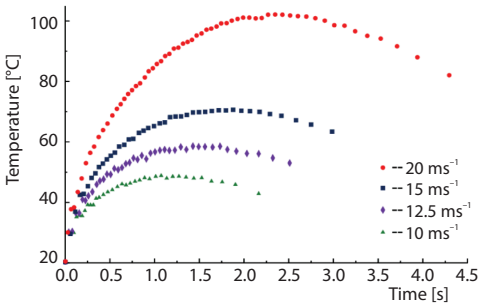

Figure 8. Surface temperature change of brake disc

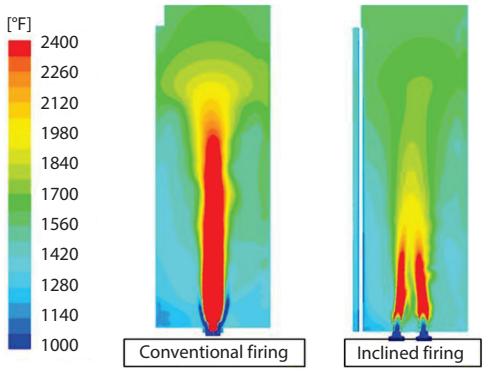

Figure 9. Heat flow distribution

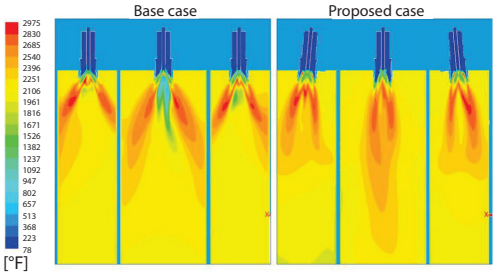

Figure 10. Temperature distribution

Conclusion

The thesis analyzes the existing methods of dealing with the sliding friction contact problem and proposes applying the constraint function method to deal with the thermal-mechanical coupling problem under the condition of sliding friction contact. The paper analyzes the contact conditions of the thermo-mechanical coupling model and gives its mathematical expression. The thesis applies the constraint function method, expresses the contact condition with a constraint equation, and proves that the constraint equation satisfies the contact condition under certain conditions. The example shows that applying the constraint function method for thermo-mechanical coupling analysis has the characteristics of good convergence and algorithm stability.

References

[1] Omrani, R., *et al*., Thermal Coupling of an Open-Cathode Proton Exchange Membrane Fuel Cell with Metal Hydride Canisters: An Experimental Study, *International Journal of Hydrogen Energy*, *45* (2020), *53*, pp. 28940-28950
[2] Mei, W., *et al*., The Effect of Electrode Design Parameters on Battery Performance and Optimization of Electrode Thickness Based on the Electrochemical-Thermal Coupling Model, *Sustainable energy & Fuels*, *3* (2019), 1, pp. 148-165
[3] Wu, S., Study and Evaluation of Clustering Algorithm for Solubility and Thermodynamic Data of Glycerol Derivatives, *Thermal Science*, *23* (2019), 5, pp. 2867-2875
[4] Bahman, A. S., *et al*., A Lumped Thermal Model Including Thermal Coupling and Thermal Boundary Conditions for High-Power IGBT Modules, *IEEE Transactions on Power Electronics*, *33* (2017), 3, pp. 2518-2530
[5] Zhou, S., *et al*., Optical Thermometry Based on Cooperation of Temperature-Induced Shift of Charge Transfer Band Edge and Thermal Coupling, *Optics Express*, *26* (2018), 21, pp. 27339-27345
[6] Ma, G. M., *et al*., Effect of Material Volume Conductivity on Surface Charges Accumulation on Spacers under DC Electro-Thermal Coupling Stress, *IEEE Transactions on Dielectrics and Electrical Insulation*, *25* (2018), 4, pp. 1211-1220
[7] Chen, M. C., *et al*., Uniform Regularity for a Keller-Segel-Navier-Stokes System, *Applied Mathematics Letters*, *107* (2019), 106476
[8] Wu, S., Construction of Visual 3-D Fabric Reinforced Composite Thermal Perfomance Prediction System, *Thermal Science*, *23* (2019), 5, pp. 2857-2865
[9] Li, H., *et al*., Thermal Coupling Analysis in a Multichip Paralleled IGBT Module for a DFIG Wind Turbine Power Converter, *IEEE Transactions on Energy Conversion*, *32* (2016), 1, pp. 80-90
[10] Tetuko, A. P., *et al*., Thermal Coupling of PEM Fuel Cell and Metal Hydride Hydrogen Storage Using Heat Pipes, *International Journal of Hydrogen Energy*, *41* (2016), 7, pp. 4264-4277
[11] Li, H., *et al*., Ratiometric Temperature Sensing Based on Non-Thermal Coupling Levels in BaZrO3 : $Yb3^{+}/Er3^{+}$ ceramics, *Optical Materials Express*, *7* (2017), 8, pp. 3003-3010

Paper submitted: November 13, 2020
Paper revised: December 22, 2020
Paper accepted: January 13, 2021